PERGAMON

Journal of Structural Geology 25 (2003) 1451–1469

JOURNAL OF STRUCTURAL GEOLOGY

www.elsevier.com/locate/jsg

Magma emplacement and mafic–felsic magma hybridization: structural evidence from the Pan-African Negash pluton, Northern Ethiopia

Asfawossen Asrat[a,b,*], Gérard Gleizes[c], Pierre Barbey[a], Dereje Ayalew[b]

[a]*CRPG-CNRS, 15, Rue Notre-Dame des Pauvres, B. P. 20, 54501 Vandoeuvre-lès-Nancy Cedex, France*
[b]*Department of Geology and Geophysics, Addis Ababa University, P.O.Box 1176, Addis Ababa, Ethiopia*
[c]*CNRS-UMR 5563 LMTG, Université Paul Sabatier, 38, rue des Trente-six-Ponts, 31400 Toulouse, France*

Received 12 January 2002; received in revised form 20 August 2002; accepted 7 September 2002

Abstract

The Negash pluton (50 km^2) consists of late Pan-African, high-K, calc-alkaline granitoids intruded into low-grade metavolcanics–metasediments. This almost circular massif consists of monzogranites, granodiorites, diorites–gabbrodiorites, and hybrid diorites. The anisotropy of magnetic susceptibility (AMS) method was used to determine internal structures of the pluton. The foliation trajectories are concentric and inward dipping. The lineation pattern displays an external zone characterised by horizontal concentrically oriented lineations and an internal zone with NW–SE oriented lineations. These petro-structural data clearly locate the feeder zone at the north-western tip of the pluton and indicate the subsequent expansion of the magmas towards the SE. The pluton is a result of in-situ assembly of four magma batches, which were forcefully injected into pre-existing foliated country rocks in relation to transpressional tectonic regime. Two types of mafic–felsic magma interactions are recognised: homogeneous and heterogeneous hybrid diorites at the north-western part, and mingled interfaces at the diorite–granodiorite contact zones mainly visible in the eastern and south-eastern parts. The in-situ mingling along diorite–granodiorite contacts was achieved at the level of emplacement during the injection of dioritic magma into the felsic magmas while the hybrid diorites are assumed to result from two-way conduit mixing and mingling during simultaneous rising of mafic and felsic magmas.
© 2003 Published by Elsevier Science Ltd.

Keywords: Ethiopia; Pan-African; Granite; Anisotropy of magnetic susceptibility (AMS); Hybridization; Pluton emplacement

1. Introduction

A systematic structural study of plutons using the anisotropy of magnetic susceptibility (AMS) coupled with petrographic interpretations has been proved to be a revealing technique in the understanding of internal structures of granitoids and in determining the tectonic regime during magma emplacement. This AMS methodology has been successfully applied with efficient results to late Neo proterozoic plutons in Madagascar (Nédélec et al., 1994), Western and Northern Africa (e.g. Ferré et al., 1995, 1997, 2002; Déléris et al., 1996; Djouadi et al., 1997) and Brazil (Archanjo, 1993; Archanjo et al., 1994). These studies indicate that most plutons are emplaced in transpressive tectonic regimes. Although there are many late Pan-African plutons in Ethiopia, such structural studies are non-existent.

The nature of mafic–felsic magma interactions (magma mixing and mingling) is an important element in the understanding of the dynamics of magma chambers and pluton emplacement. Most previous works generally agreed on the replenishment of a felsic magma chamber by intruding mafic magmas as the major process responsible for the hybridization (mixing and mingling) of magmatic rocks (e.g. Reid et al., 1983; Whalen and Currie, 1984; Barbarin, 1988; Zorpi et al., 1989; Michael, 1991; Didier and Barbarin, 1991 and references therein; Bateman, 1995; Wiebe, 1996; Wiebe and Adams, 1997; Snyder and Tait, 1998; Wiebe and Collins, 1998; Poli and Tommasini, 1999), while some works indicate that the intrusion of felsic magmas into mafic chambers may be more common than so far realised (e.g. Wiebe and Wild, 1983; Wiebe, 1987; Weinberg, 1997; Weinberg and Leitch, 1998). Others consider dynamic, two-way conduit mixing and hybridization along rising and during emplacement of magmas as equally important processes (e.g. Oldenburg et al., 1989; Castro et al., 1995; Seaman et al., 1995).

* Corresponding author. Tel. +251-1-55-32-14, fax. +251-1-55-23-50.
E-mail address: asrata@ged.aau.edu.et (A. Asrat).

0191-8141/03/$ - see front matter © 2003 Published by Elsevier Science Ltd.
PII: S0191-8141(02)00182-7

Here, we report on the Negash pluton (northern Ethiopia; Fig. 1), which displays numerous spectacular mafic–felsic magma interactions. This study is based on a systematic structural investigation of the pluton using the AMS coupled with detailed field and petrographic studies. The different mafic–felsic magma interactions are characterised by distinct structural patterns, which are used to understand how various types of interactions between mafic and felsic magmas occurred with respect to aggregation of the magma batches and pluton growth.

2. Geological setting

The Northern metamorphic terrain of Ethiopia is represented by a series of thick, inhomogeneous volcano-sedimentary assemblages, which belong to the Arabian–Nubian Shield (ANS) sector of the East Pan-African orogen (Stern and Dawoud, 1991; Tadesse et al., 1999; Asrat et al., 2001). This terrain is dominantly characterised by steeply dipping and extensively folded, low-grade metamorphic rocks intruded by various granitic and mafic intrusions (Asrat, 1997; Tadesse, 1997; Alemu, 1998; Tadesse et al., 2000). This terrain is considered to be formed by lateral crustal growth through processes of arc and terrane accretion during the Pan-African (950–500 Ma) orogenic event (Almond, 1983; Kröner et al., 1987, 1991; Stern and Dawoud, 1991; Stern, 1994; Asrat, 1997) where granitic magmatism played an important role.

The metamorphic sequence in the Mekele–Adigrat area (Fig. 1a) is composed dominantly of heterogeneous metavolcanics (breccias, agglomerates, bedded tuffs and lavas) all inter-bedded with subordinate marine clastics, rare limestones, tuffaceous slates, redeposited ash, and grey-wackes composed partly of volcanic fragments, exhibiting considerable lateral variations. The sequence, with a thickness reaching up to 2500 m in some sections, is metamorphosed to greenschist facies except in contact aureoles of plutons. The regional foliation oriented N–S to NNE–SSW appears to have been produced by pervasive shortening during D_1 deformation (Alene, 1996). D_2 deformation is represented by the development of semi-ductile dextral shear zones.

Felsic plutonism of variable age and lithology is a characteristic feature of this metamorphic terrain where syntectonic, late- and post-tectonic granitoids have been identified (e.g. Beyth, 1972; Garland, 1980; Asrat, 1997; Tadesse, 1997; Alemu, 1998). The syntectonic bodies are medium grained epidotized, foliated granites (rarely granodiorites) elongated along the regional strike. The late- to post-tectonic plutons consist of granites, monzo-granites, granodiorites, tonalites, monzonites often accompanied by diorites and gabbrodiorites, and cut by many late stage aplite and quartz porphyry dikes. From K–Ar (Miller et al., 1967; Garland, 1980) and Ar–Ar ages (Mock et al., 1999), the late- to post-tectonic granitoids in this area are considered to be Upper Proterozoic to Lower Palaeozoic (660–540 Ma).

3. The Negash pluton

The Negash pluton, an almost circular body of 8 km diameter and about 50 km^2 outcrop area (Fig. 1b), has long been considered as a post-tectonic granitoid (e.g. Beyth, 1972; Kazmin, 1972; Garland, 1980). Its emplacement age is not well-defined because the only available age (676–589 Ma) is based on Ar–Ar dating on micas (Mock et al., 1999). The pluton is a high-K, calc-alkaline, metaluminous, I-type granitoid (Asrat, 1997). It forms a depressed trough bounded by hills of metavolcanics and metasediments and its outline mostly follows the foliation trajectories in the country rocks of the contact aureole. The foliation trajectories of the country rocks strike N–S dipping at steep angles towards the west. The western contact of the Negash pluton runs along the Suluh shear zone (Fig. 1b; Asrat, 1997), which is responsible for the pervasive deformation of brecciated mafic metavolcanics. Close to the pluton, all the foliation trajectories are deflected around it and perfectly wrap it in map view forming two asymmetric triple points at the southern and north-western parts of the pluton. Numerous septa of country rocks within the pluton are in distinct structural continuity with the surrounding country rocks. These country rocks are strongly flattened at the eastern and western borders close to the pluton and N–S oriented, horizontal stretching lineations with dextral sense of shear can be observed in these areas.

Systematic oriented core sampling has been conducted on the whole pluton. Detailed petrographic determinations were carried out on thin-sections prepared from these core samples and from geochemical samples. In order to determine the structure of the pluton, a magnetic susceptibility study was performed on the oriented core samples. In addition, systematic planar fabric measurements were carried out mainly on flattened mafic enclaves at each core site.

3.1. Rock types and microstructures

The Negash pluton displays a crescent-shaped inward lithological zonation of: (a) monzogranite, (b) granodiorite to tonalite, (c) magnetite-rich diorite to gabbrodiorite, and

Fig. 1. (a) Geological setting of the Northern metamorphic terrain of Ethiopia (modified after EIGS, 1997; Tadesse et al., 1999; Asrat et al., 2001). The eastern sector of the terrain corresponds to the Mekele–Adigrat area. Open square shows the Negash area. (b) Geological sketch map of the Negash area with the location of the AMS sampling stations in the Negash pluton.

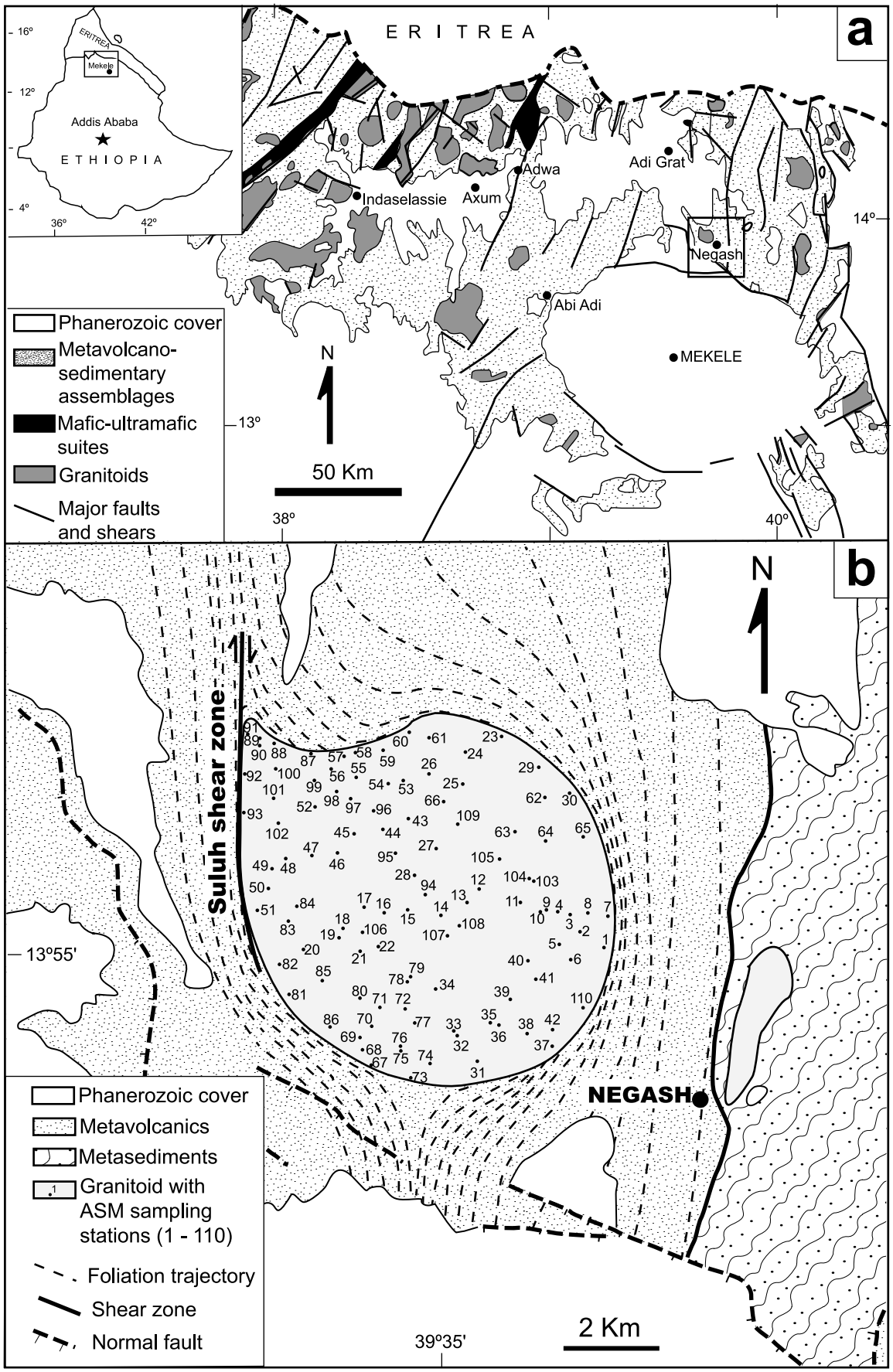
a
ERITREA
Mekele
Addis Ababa
ETHIOPIA
16°
12°
4°
36°
42°
Adwa
Adi Grat
Indaselassie
Axum
Negash
Abi Adi
MEKELE
14°
13°
38°
40°
N
50 Km
Phanerozoic cover
Metavolcano-sedimentary assemblages
Mafic-ultramafic suites
Granitoids
Major faults and shears
b
N
Suluh shear zone
13°55'
39°35'
NEGASH
2 Km
Phanerozoic cover
Metavolcanics
Metasediments
Granitoid with ASM sampling stations (1 - 110)
Foliation trajectory
Shear zone
Normal fault

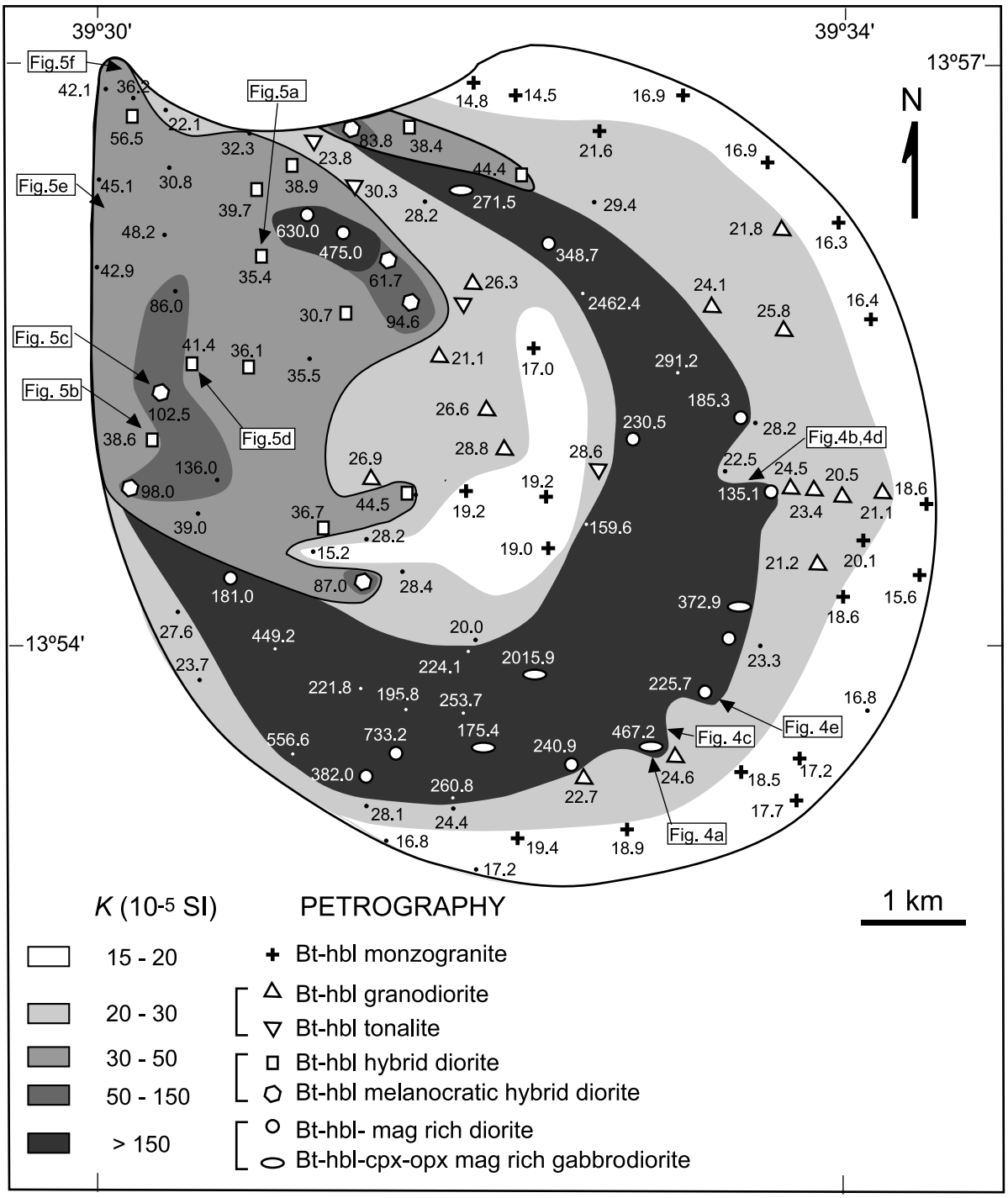

Fig. 2. Petrographic and susceptibility map of the Negash pluton. The dots are AMS sampling stations. *K* is the bulk susceptibility value. Locations of photographs in Figs. 4 and 5 are marked.

(d) mesocratic to melanocratic hybrid diorite, although the zonation is more complex towards the centre of the pluton (Fig. 2). The monzogranites and granodiorites–tonalites form separate low hills of conspicuously horizontally and vertically jointed blocks, while the mafic and hybrid rocks outcrop as massive bodies and rarely as chaotic boulders. Radial and concentric pegmatites, aplites and quartz porphyry dikes and quartz veins cut all the facies. The monzogranites, granodiorites and tonalites consist of quartz, alkali feldspar, plagioclase, biotite and hornblende (Fig. 3a and b). The diorites and gabbrodiorites are composed of plagioclase, biotite, hornblende, rare phlogopite, with some clino- and orthopyroxene in the gabbrodiorite (Fig. 3c). The hybrid diorites are composed of plagioclase, biotite and hornblende, rare quartz, alkali feldspar, phlogopites and traces of oxide (Fig. 3d). Sphene, apatite, zircon and seldom

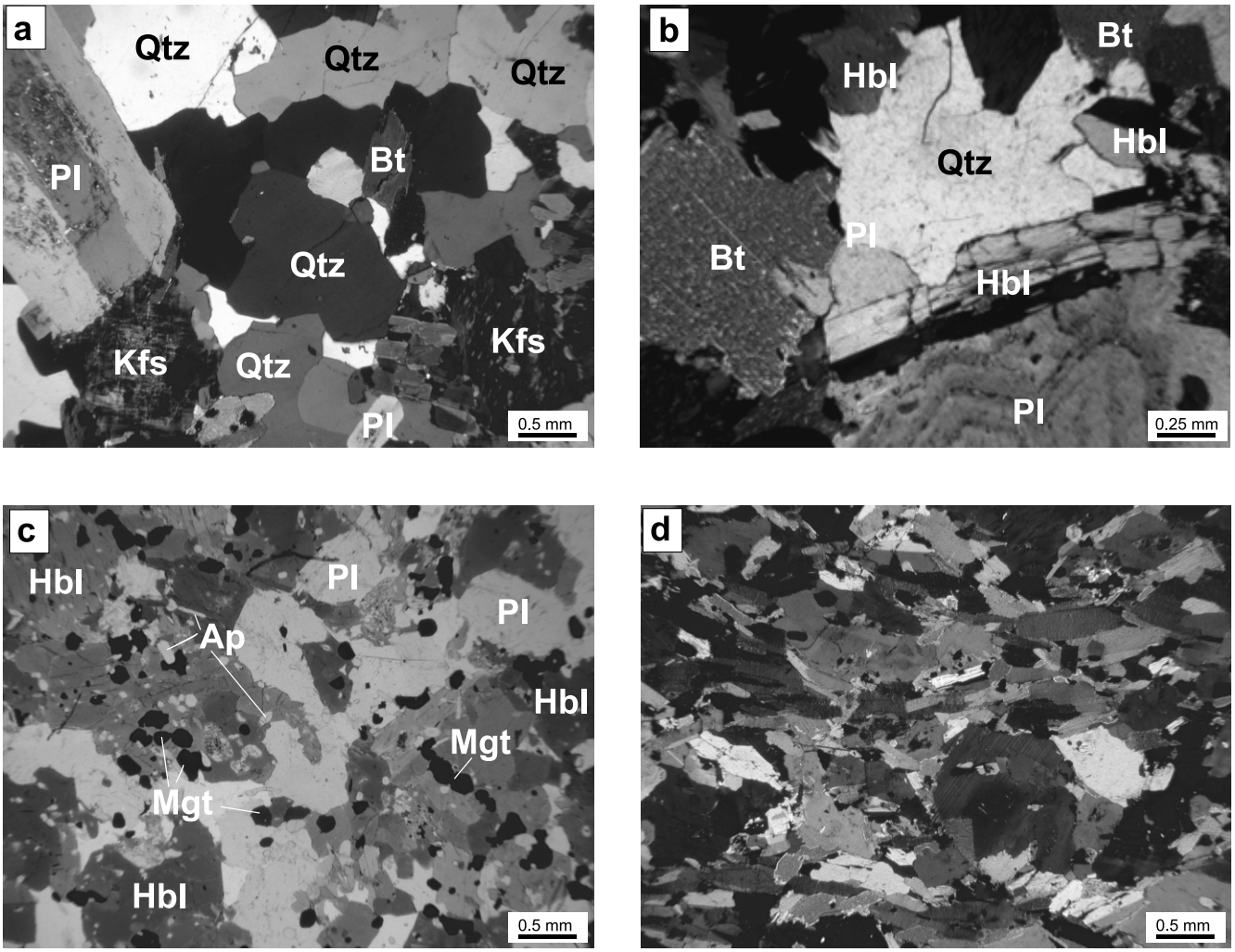

Fig. 3. Photomicrographs of: (a) a monzogranite with magmatic microfabrics containing interstitial K-feldspar and quartz, zoned plagioclase and subhedral biotite and hornblende; (b) a granodiorite with magmatic microfabrics: equigranular, zoned plagioclase, interstitial quartz, and euhedral to subhedral biotite and hornblende; (c) a gabbrodiorite containing high proportions of magnetite and apatite grains with cumulate character; (d) a hybrid diorite from close to the western border of the pluton (the magmatic high strain zone), showing a preferred N–S orientation (parallel to the scale bar) but displaying magmatic microfabrics without any subsolidus deformation.

epidote and calcite are common accessories in all the petrographic types, but the hybrid diorites are significantly richer in sphene.

In the monzogranites, granodiorites and tonalites, the plagioclase cores are rarely retrogressed to sericite, calcite and epidote; some biotites are altered to epidote and chlorite at their borders. In the diorites and gabbrodiorites, the plagioclases are slightly retrogressed. The hybrid diorites in the north-western part of the pluton are distinct in that they are affected by a pervasive hydrothermal alteration (expressed by chlorite + sericite + epidote paragenesis) especially at the contact with the diorites. The plagioclases are highly retrogressed to epidote, sericite, muscovite and calcite. The amphiboles are also partly transformed to epidote.

A systematic microstructural study on core samples indicates that the Negash pluton rocks are characterised almost exclusively by magmatic microstructures with limited near-solidus deformation (Fig. 3; for definitions see Bouchez et al., 1981, 1992; Vernon et al., 1988; Paterson et al., 1989). In some cases, high-temperature, near-solidus deformation can be observed: kinked biotites, rarely broken plagioclases, and locally sub-grains in quartz (chess-board microstructures). Close to the western border of the pluton, the hybrid diorites display a preferred N–S orientation but the microstructures show magmatic fabric without any subsolidus deformation (Fig. 3d). This zone in the pluton is, therefore, a magmatic high strain zone.

3.2. Hybridization

The Negash pluton displays spectacular mafic–felsic magma interactions (mixing and mingling). Two major types of interactions are observed in two major zones of the pluton: (i) mingled and mixed mafic–felsic interfaces between the diorites and granodiorites, especially visible

at the eastern and south-eastern parts of the pluton (Fig. 4); and (ii) intensely mingled and hybrid diorites, which constitute the NW part of the pluton (Fig. 5). In addition, numerous swarms of relatively small-sized mafic enclaves are dispersed in the monzogranites and granodiorites that constitute the rest of the pluton.

Magma interactions at the diorite–granodiorite lower interface are characterised by extensive hybridization (both mixing and mingling). Several types of in situ mingling structures show that this lower contact was mechanically unstable (Fig. 4):

(i) lobate contact with interfingering of diorites into granodiorites at decametric scale (Fig. 4a) is a prominent feature at the south-eastern contact zone;
(ii) abundant small 'incipient' pipes (Fig. 4b) and larger granitic pipes (Fig. 4c), breccia dykes (composed of angular dioritic blocks within a granitic matrix) and veins cut through the diorites; some of these veins are strongly enriched in K-feldspar phenocrysts (Fig. 4d), which may also be found in hybridized diorites (Fig. 4e); the granitic pipes, a few centimetres to 30 cm in diameter, are locally inclined or near horizontal;
(iii) numerous swarms of elliptical mafic enclaves within the granodiorites above the dioritic mass; these enclaves at the upper interface are generally rounded and slightly elliptical.

Two types of mafic–felsic interactions are observed in the north-western part of the pluton: (i) mixing and mingling structures similar to those observed in the granodiorite–diorite interface at the south-eastern part of the pluton (Fig. 5d–f) characterised by rounded enclaves; and (ii) hybrid diorites characterised by both mixing and mingling with high enclave to granite ratio, and by flattened and stretched enclaves (Fig. 5a–c), without any way up structures.

The hybrid diorites often form separate low hills of strongly horizontally jointed blocks. Fig. 5a shows one of such hills where oblique layering between dark diorite and light-coloured granodiorite is observed. Close to the western border of the pluton, the hybrid rocks are represented by metre scale alternation of mafic and felsic material in nearly equal proportions forming a vertical N–S layering. Fig. 5b and c represent this kind of layering in a horizontal view perpendicular to the layering and parallel to the lineation (*XZ* section). Horizontal mineral stretching lineations can be observed on the foliation planes. Traces of mafic–felsic interactions similar to those at the granodiorite–diorite interfaces are shown by swarms of mafic enclaves within granodioritic magma, where the enclaves can be rounded (Fig. 5d and e) or angular and fractured (Fig. 5f) as a function of the relative temperature and rheology of the dioritic and granodioritic magmas (Fernandez and Gasquet, 1994). Fig. 5d shows hybridized mafic enclaves (note the high amount of K-feldspar xenocrysts) enclosed within a more felsic hybridized diorite. The asymmetry of the mafic enclave at the centre of the photograph in Fig. 5b indicates a dextral sense of shear.

4. AMS study

4.1. Methodology

The AMS technique has proved to be a powerful method for determining the fabrics of poorly anisotropic granitoids and this kind of study is routinely applied in many plutons all over the world with efficient results (e.g. Benn et al., 1993; Archanjo et al., 1994; Bouchez et al., 1997 and references therein; Saint-Blanquat and Tikoff, 1997; Gleizes et al., 1998, 2001; McNulty et al., 2000). The AMS is a reliable method because the AMS ellipsoid of granitic samples, defined by its three main axes $K_1 \geq K_2 \geq K_3$, characterises the magnetic fabric of these rocks. In the case of paramagnetic granitoids where the conspicuous mafic minerals are biotite and amphibole, the long axis K_1, called the magnetic lineation, is parallel to the zone axis of the biotites and to the mean elongation of the amphiboles; and the short axis K_3, normal to the magnetic foliation, is the mean preferred planar orientation of biotites and amphiboles. In ferromagnetic rocks, however, the AMS is related to the shape anisotropy of magnetite, which generally depicts the fabric of the rocks (Archanjo et al., 1995; Grégoire et al., 1998).

The magnetic susceptibility of the granitoids was determined from 110 sampling stations regularly distributed over the pluton (Fig. 1b). Two oriented cores, about a few metres apart, were drilled from each station. In the laboratory, two to three specimens (cylinders with $d = 25$ mm and $h = 22$ mm) were cut from each core. Each specimen was measured for its AMS at low field (4×10^{-4} T) using a Kappabridge KLY-2 susceptometer (Geofyzika Brno). Measurements result in the magnitude and orientation of the three main axes $K_1 \geq K_2 \geq K_3$ of the magnetic susceptibility ellipsoid with a good consistency among samples from the same station. The bulk susceptibility value, K [$= (K_1 + K_2 + K_3)/3$], for each station is, therefore, an average of at least four

Fig. 4. Hybridization features at the eastern and south-eastern diorite–granodiorite contact zone. The locations of the photographs are marked in Fig. 2. (a) Interfingering of dioritic lobes into the granodiorites. The broken lines outline the contacts and the location of (c) is marked by an arrow. (b) Evidence of melt instability at the base of a fragmented mafic layer with small incipient pipes. (c) Inclined granitic pipes in diorites, the direction of warping is parallel to the lineation. (d) Remnants of granodioritic veins and veinlets in the diorites outlined by accumulation of large K-feldspar crystals. (e) Xenocrysts of K-feldspar in the diorites.

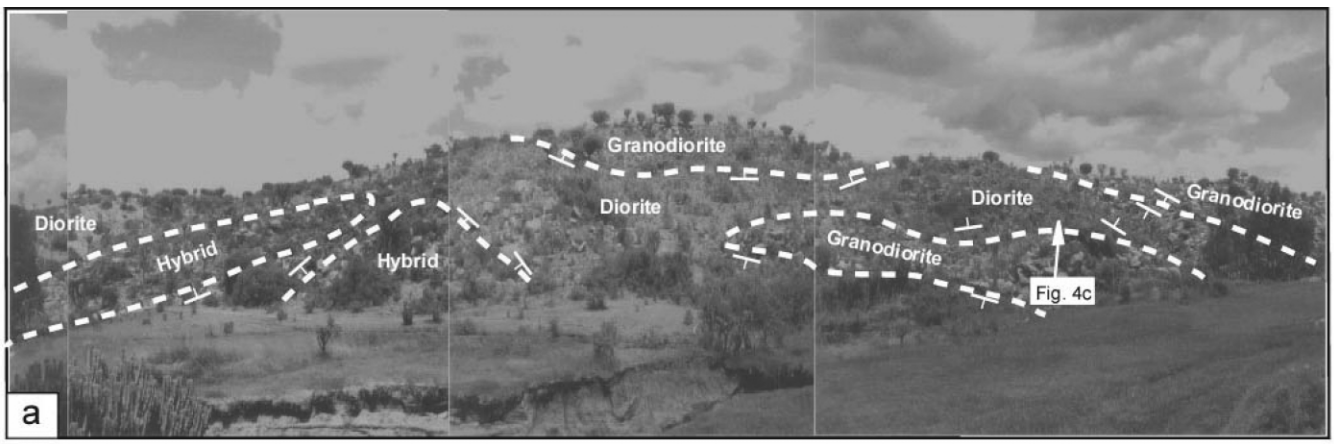
Granodiorite
Diorite
Diorite
Hybrid
Hybrid
Diorite
Granodiorite
Granodiorite
Fig. 4c
a

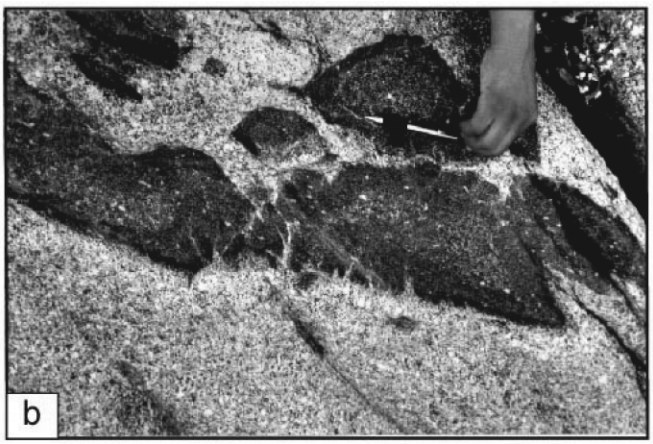
b


c
6 cm

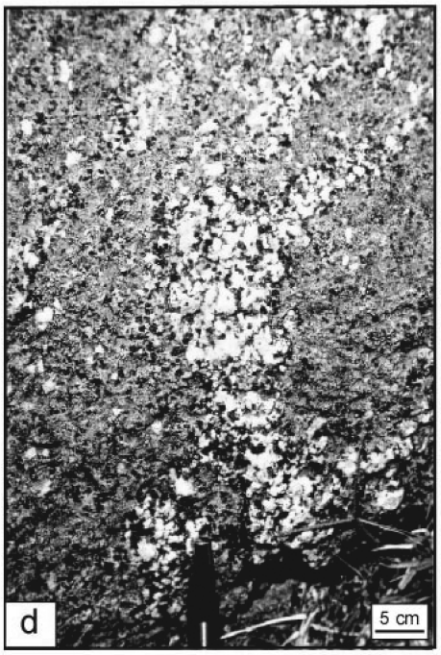
d
5 cm

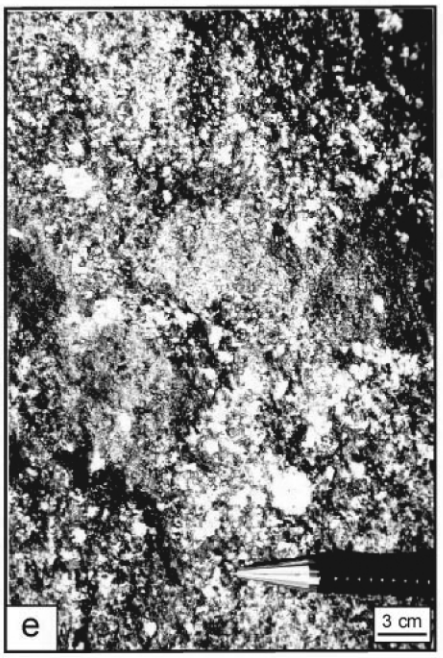
e
3 cm

individual measurements. The total anisotropy (Ppara%) and shape parameter (T) are respectively determined by the relations $\text{Ppara\%} = 100[(K_1/K_3) - 1]$ and $T = [2(\ln K_2 - \ln K_3)/(\ln K_1 - \ln K_3)] - 1$. The results of the AMS measurements are given in Table 1.

4.2. Magnetic susceptibility and rock types

K values range from 15×10^{-5} SI to 2462×10^{-5} SI. This large difference in magnetic susceptibility indicates that the pluton is composed of both paramagnetic and ferromagnetic rock types, in agreement with the petrography. For instance, the monzogranites, granodiorites, tonalites and hybrid diorites are composed mainly of paramagnetic minerals (biotite and hornblende) and traces of magnetite (Fig. 3a, b and d). In this case, K is low and directly related to the iron content and thus to the petrographic type (Rochette et al., 1992; Gleizes et al., 1993). The diorites and gabbrodiorites, on the other hand, contain magnetite, which is a ferromagnetic mineral that results in high susceptibility values ranging between 200 and 400×10^{-5} SI, for most of the samples. The highest values ($K > 500 \times 10^{-5}$ SI) correspond to gabbrodiorites whose petrography confirms the high proportions of magnetite grains in relation to a cumulate character (Fig. 3c). The susceptibility and petrographic map (Fig. 2) reveals an almost perfect correlation between the susceptibility values and the petrographic types defined from independent thin section analysis.

4.3. Field planar fabrics and magnetic foliations

Planar fabrics were systematically determined at each core site in the pluton from flattened mafic enclaves and from the metamorphic septa. Foliation measurements were also conducted on the surrounding country rocks.

The trajectories of the planar fabrics of the mafic enclaves follow a pattern parallel to the contour of the pluton (Fig. 6a) and converge towards its north-western tip. The dip is vertical to sub-vertical at the south-eastern border of the pluton, decreases towards the centre and then increases in the NW part. The septa and their planar fabrics follow a general pattern defined by the fabric of mafic enclaves. However, at the northern and south-western borders of the pluton, there is a general obliquity between the two respective patterns. The foliation trajectories in the country rocks follow the outline of the pluton except in the N and SSW, exactly where the planar fabrics of the septa are oblique to those of the mafic enclaves. These angular unconformities between the septa and foliation patterns in the granitoids indicate the sense of movement (expansion) of the magma towards the SE. The septa are the continuation of the country rocks into the pluton as demonstrated in the northern part, where the country rocks with foliations oblique to the contour of the pluton are continued into the pluton in the form of the septa.

The trajectories of the magnetic foliations are nearly in complete agreement with the independently determined field planar fabrics, and show a very distinct, almost concentric, inward pattern in map view, following the contour of the pluton (Fig. 6b). Although this pattern is generally parallel to the lithological zonation, the foliations cut across the various facies in the northern part of the pluton. A stereographic plot of poles to foliations shows a mean foliation dipping towards the SW, although the foliations in the south-western half of the pluton are steeply dipping towards the NE. All along the zone of high strain at the western border of the pluton, the foliation planes are vertical and oriented almost N–S parallel to the western contact (Fig. 5b and c). Along the contact between the diorites and the granodiorites at the south-eastern part of the pluton the foliation trends perfectly follow the plan of the contact even when interfingering of the diorites into granodiorites occurs (Fig. 2). In conclusion, the three-dimensional shape of the pluton can be envisaged as an elliptical funnel-shaped body with an axis striking NW–SE and with its tip located at its north-western part.

4.4. Magnetic lineations

The magnetic lineations show more complicated but interesting patterns allowing three distinct zones to be identified (Fig. 7):

1. The external zone of the pluton displays circumferential lineations that are almost horizontal to sub-horizontal. However, lineations at the northern border and at the western border (the high-strain zone) are slightly plunging to the north-western tip of the pluton.
2. The internal zone of the pluton shows lineations that have more uniform orientations towards the NW with a mean value of 292°/33°. This mean lineation trend is parallel to the NW–SE axis of the pluton defined above by the foliation pattern. An interesting point is that along the mingled interface between the diorites and the granodiorites in the south-eastern part of the pluton, the

Fig. 5. Hybrid diorites constituting the north-western part of the Negash pluton. The locations of the photographs are marked in Fig. 2. (a) A hybrid diorite hill with horizontal joints, and oblique interlayering of mafic and felsic rocks. (b) Hybrid diorite from the high strain zone in the western border of the pluton, with stretched mafic enclaves indicating a dextral sense of shear (half arrows); the photograph is perpendicular to the vertical foliations and parallel to the horizontal lineations both oriented N–S (*XZ* section). (c) Foliated, vertical N–S striking layering of mafic–felsic masses in nearly equal proportions, at the western border of the pluton (*XZ* section). (d) Light-coloured hybrid diorites containing non-deformed, rounded mafic enclaves with weak fabric. (e) and (f) Hybrid diorites from the feeder zone with rounded and broken, angular mafic enclaves, respectively, enclosed in granodioritic matrix.

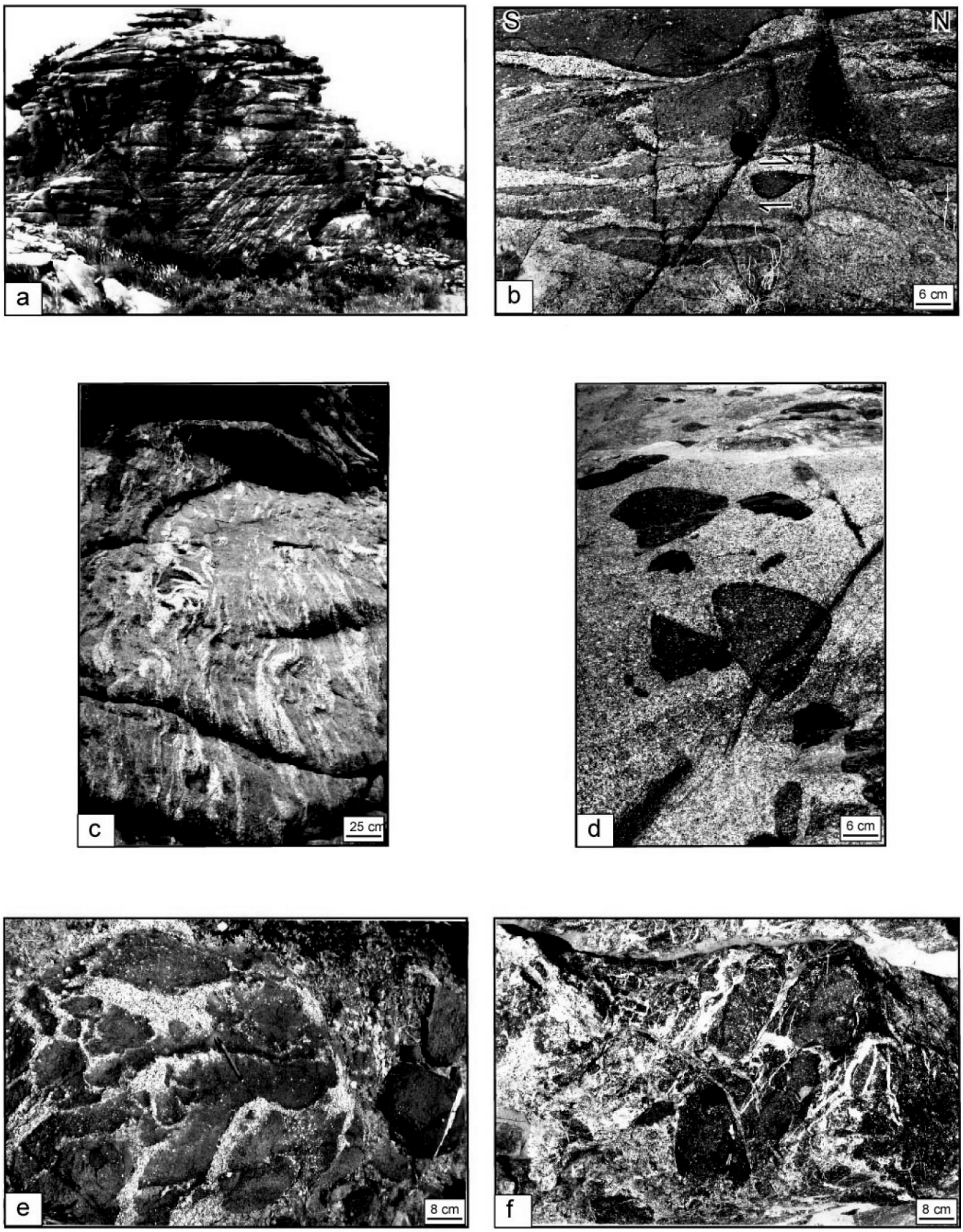
a
S
N
b
6 cm
c
25 cm
d
6 cm
e
8 cm
f
8 cm

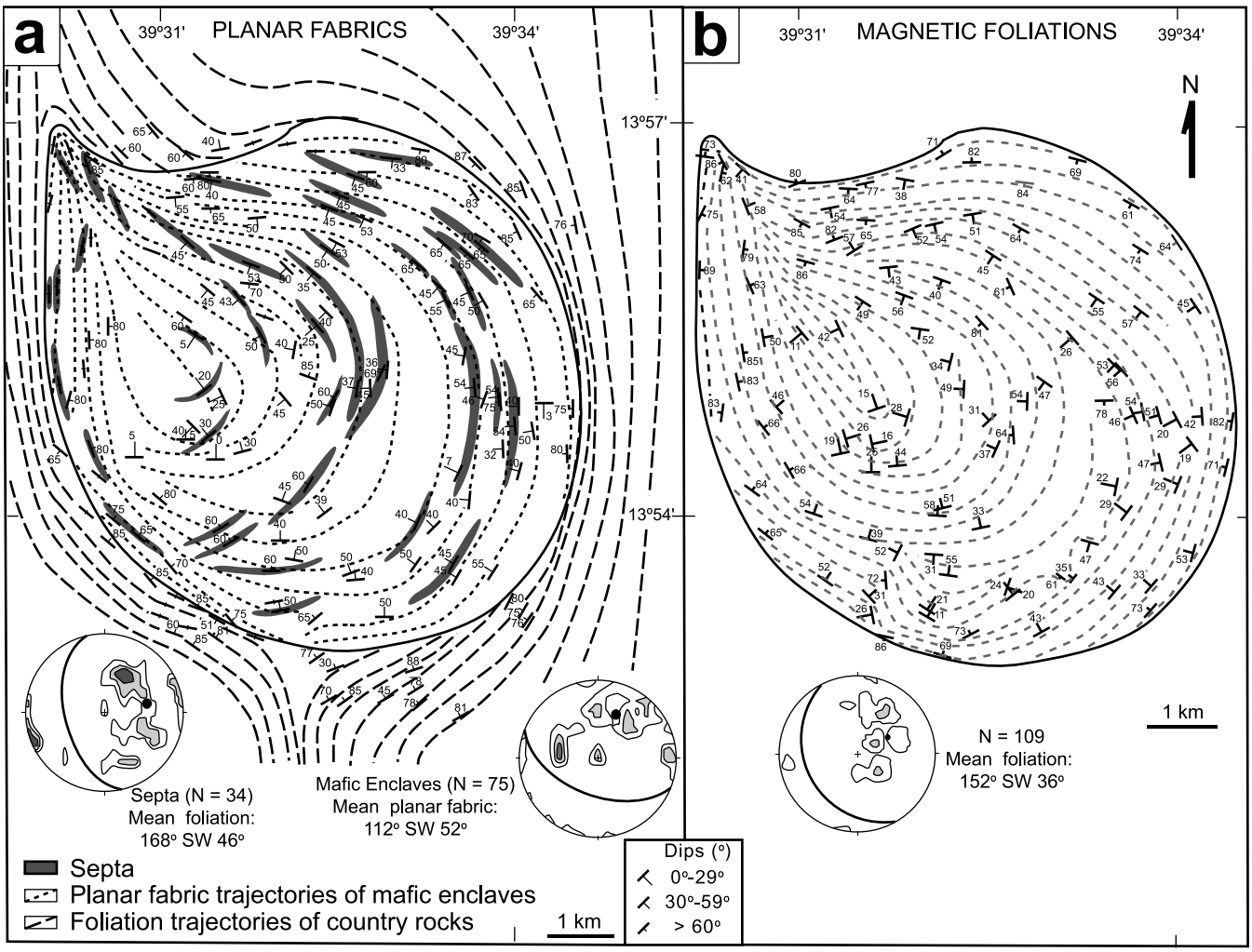

Fig. 6. (a) Map of planar fabrics determined from field measurements in the country rocks and from mafic enclaves and septa in the Negash pluton, and stereographic plots of the poles of the foliations of the septa and planar fabrics of the mafic enclaves. (b) Map of magnetic foliations and foliation trajectories, and stereographic plot of the foliation poles. (Stereonets: Schmidt lower hemisphere; 1% area contours; N = number of measurements).

lineations in the granodiorites are horizontal and follow the contour of the pluton while the lineations in the diorites are oriented towards the NW at relatively higher plunges (in agreement with the foliation patterns in the same zone, as discussed later in Section 5.3).

3. The northern and south-western parts of the pluton where two smaller zones display lineation patterns markedly at discordance from the rest of the pluton. In the northern part, the magnetic lineations are all oriented towards the south with relatively higher plunges (mean lineation at 177°/51°), while in the south-western part, they are all inclined towards the NE with similar plunges (mean lineation at 36°/53°).

4.5. Magnetic anisotropy

In paramagnetic granites, magnetic anisotropy is specifically defined as Ppara%, which depends on the preferred orientation of the minerals, hence the intensity of the rock fabric, which is related to the deformation. This has been previously demonstrated by comparison with microstructures (e.g. Gleizes et al., 2001). Generally, Ppara% values do not exceed 5% except in shear zones. In ferromagnetic granites, however, the magnetic anisotropy is more difficult to interpret because it is mainly linked to the shape and amount of magnetite grains, and often the anisotropy values may reach up to 10–30% (Borradaile, 1988; Rochette et al., 1992; Bouchez, 1997).

In the Negash pluton, there are both para- and ferromagnetic rocks and the anisotropy ranges from 0.5 to 15.5% (Fig. 8a):

1. The highest values (>10%) are restricted to the diorites and gabbrodiorites, and this is related to their highly ferromagnetic nature.
2. The Ppara% = 5–10% are distributed in bifurcated structures with E–W and NNW–SSE bands that merge towards the north-western tip of the pluton. These bands cross most of the rock types and correspond in the field to rocks with strong fabrics,

Table 1
AMS data for the 110 sampling stations in the Negash pluton. (K = magnetic susceptibility magnitude; K_1 = azimuth and plunge of the magnetic lineation (in degrees); K_3 = azimuth and plunge of the pole of the magnetic foliation; Ppara% = anisotropy magnitude; T = shape parameter; * = a non-reliable, discarded measurement)

Site	K (10^{-5} SI)	K_1	K_3	Ppara%	T
1	15.8	192/11	101/28	2.6	0.00
2	20.1	187/14	53/71	2.3	−0.05
3	20.5	207/16	62/70	2.4	0.48
4	23.2	270/52	74/38	2.8	0.66
5	21.0	327/25	77/45	3.1	0.68
6	18.4	310/24	114/65	1.5	0.20
7	18.6	9/10	100/8	1.9	0.49
8	21.1	214/25	75/60	1.4	0.14
9	24.5	291/39	80/36	2.9	0.20
10	135.1	243/46	66/44	2.9	0.47
11	22.5	265/10	359/12	2.3	0.23
12	230.5	152/27	44/42	2.1	−0.20
13	28.6	314/44	92/36	2.3	0.52
14	19.2	10/21	137/59	1.5	−0.17
15	19.2	*	*	0.8	−0.06
16	44.5	315/26	107/62	0.5	0.13
17	26.9	306/12	161/75	2.3	0.14
18	36.7	348/7	253/64	2.1	0.42
19	15.6	359/19	168/71	5.3	0.08
20	181.0	353/37	240/24	6.9	0.20
21	87.0	341/24	180/65	2.6	0.41
22	28.4	285/19	175/46	3.4	0.49
23	16.9	274/28	15/21	1.9	0.27
24	21.6	99/12	7/6	2.9	0.35
25	29.4	152/41	29/26	9.3	0.68
26	44.4	173/50	351/39	1.0	0.63
27	17.0	300/64	48/9	1.8	0.59
28	26.6	263/32	104/56	3.5	0.53
29	16.9	123/3	29/29	1.8	0.51
30	16.3	179/47	57/26	1.7	0.32
31	18.9	38/21	151/47	2.8	0.54
32	22.7	*	142/66	3.3	0.40
33	240.9	57/11	289/70	2.3	−0.34
34	2015.9	284/16	168/57	*	0.38
35	467.2	297/21	36/29	2.4	−0.19
36	24.6	235/12	128/55	1.3	0.59
37	17.7	33/15	131/17	2.4	0.66
38	18.5	15/15	130/47	3.6	0.71
39	225.7	267/20	16/43	4.1	−0.45
40	372.9	285/22	101/68	4.5	−0.03
41	23.3	223/2	127/61	1.6	−0.01
42	17.2	273/29	131/57	1.9	0.18
43	26.3	197/40	20/50	4.1	0.01
44	94.6	259/38	20/34	2.7	0.38
45	30.7	248/44	33/41	4.2	0.81
46	35.5	316/17	65/48	2.9	0.58
47	36.1	271/9	50/79	0.9	−0.10
48	41.4	353/5	260/40	0.7	−0.05
49	102.5	349/7	261/5	5.4	0.54
50	38.6	350/14	258/7	7.1	0.54
51	98.0	196/31	98/10	3.5	0.35
52	35.4	284/15	15/4	7.1	0.72
53	271.5	174/55	347/36	*	0.33
54	28.2	172/52	337/38	5.9	0.47
55	30.3	171/68	3/25	2.8	0.07
56	38.9	238/28	349/36	1.1	0.06
57	23.8	117/39	3/26	2.1	0.44
58	83.8	240/46	348/13	4.1	0.00
59	38.4	250/21	10/52	1.7	0.27
60	14.8	242/27	148/19	1.8	−0.01
61	14.5	89/5	179/8	2.6	0.41
62	21.8	134/33	32/16	2.5	0.52
63	24.1	254/48	34/35	4.5	0.44
64	25.8	141/19	37/33	4.9	0.61
65	16.4	159/11	56/45	2.6	0.34
66	348.7	276/23	33/45	4.0	0.61
67	16.8	100/14	12/4	3.9	0.40
68	28.1	184/6	79/64	*	0.89
69	382.0	50/55	179/23	3.8	−0.68
70	733.2	341/19	86/18	*	0.23
71	195.8	290/44	117/38	5.1	0.23
72	253.7	99/5	4/59	7.5	0.33
73	17.2	55/63	197/21	2.3	0.74
74	19.4	3/69	152/17	2.5	0.49
75	24.4	9/9	210/79	4.3	0.61
76	260.8	66/17	213/69	2.3	−0.02
77	175.4	279/0	188/35	4.7	0.29
78	224.1	279/9	184/32	6.3	0.29
79	20.0	340/58	166/39	1.6	0.19
80	221.8	327/28	195/51	5.4	0.32
81	23.7	26/71	218/25	3.7	0.62
82	27.6	322/29	216/26	3.4	0.89
83	39.0	39/65	232/24	7.1	0.56
84	136.0	335/10	229/44	4.8	0.16
85	449.2	350/46	199/36	5.7	0.57
86	556.6	53/45	215/38	5.5	0.00
87	47.1	256/37	158/10	7.1	0.38
88	22.1	282/23	41/49	5.8	0.92
89	36.2	170/69	62/4	1.9	0.47
90	56.5	21/16	283/28	1.7	0.70
91	42.1	68/43	188/17	1.2	−0.12
92	45.1	33/26	296/15	3.3	−0.09
93	42.9	2/21	272/1	6.2	0.53
94	28.8	193/9	93/41	3.1	0.65
95	21.1	243/36	8/38	5.7	0.79
96	61.7	193/43	354/47	5.2	0.09
97	475.0	281/44	148/33	7.8	0.56
98	629.9	259/52	159/8	9.0	−0.08
99	39.7	295/37	29/5	5.0	0.46
100	30.8	140/31	248/32	3.7	0.44
101	48.2	189/1	278/11	4.1	0.72
102	86.0	151/14	246/27	5.6	−0.05
103	28.2	301/25	48/34	2.2	0.18
104	185.3	178/36	44/37	4.6	0.85
105	291.2	258/23	49/64	5.7	0.82
106	28.2	12/7	258/74	3.7	0.58
107	19.0	335/28	114/53	2.9	0.16
108	159.6	336/36	86/26	*	0.80
109	2462.4	302/46	66/29	*	0.59
110	16.8	341/40	105/37	1.0	0.17

especially in the western band (see photographs in Fig. 5a–c, marked in Fig. 8a). Since the microfabrics are magmatic in the whole pluton, these high anisotropy bands do not correspond to subsolidus deformation. Neither do they correspond to ferromagnetism, since the largest part of the rocks represented by these bands are paramagnetic. These

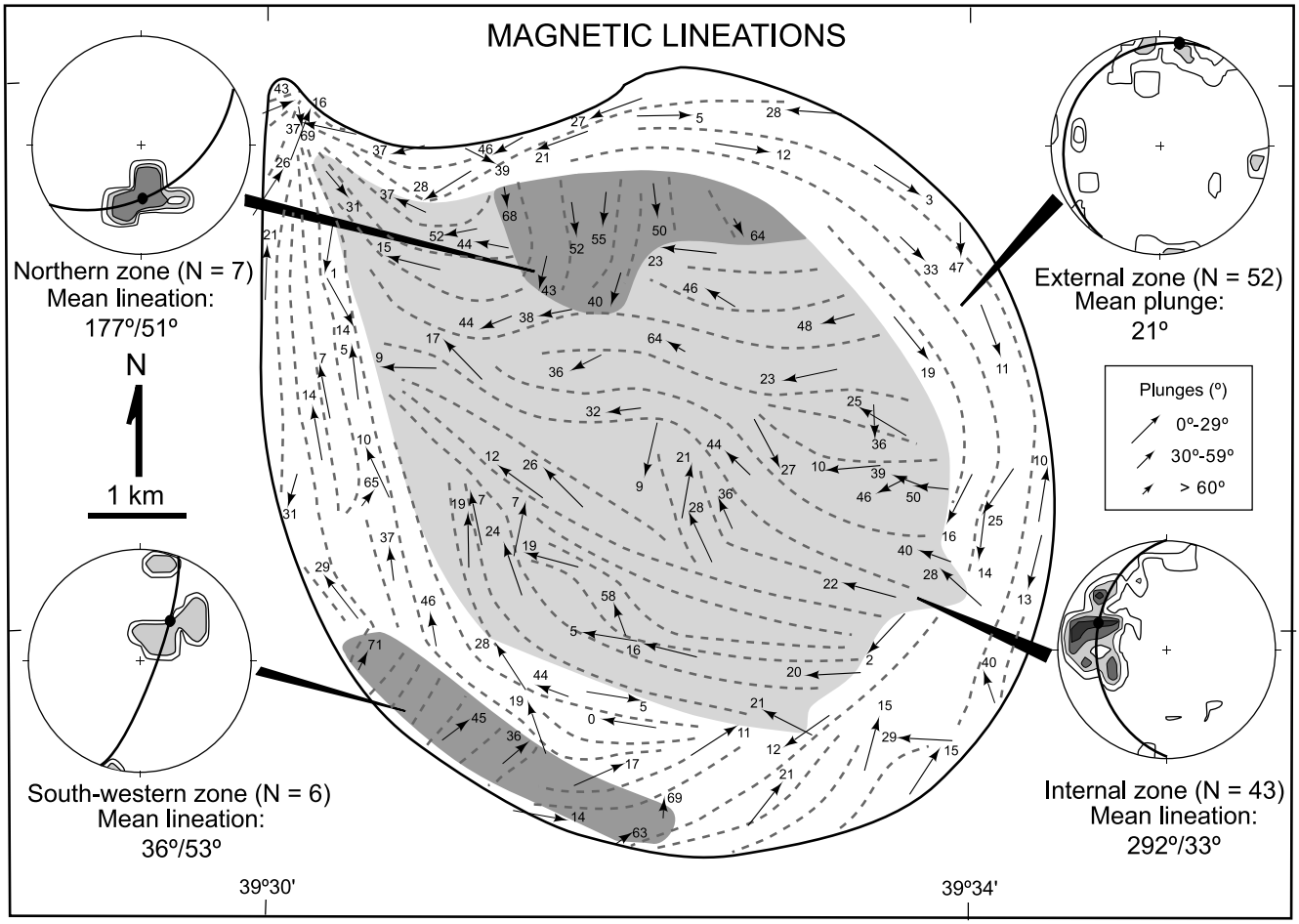

Fig. 7. Map of magnetic lineations and lineation trajectories in the Negash pluton, and stereographic plots of the lineations (Stereonets: Schmidt lower hemisphere; 1% area contours; N = number of stations). Unshaded: the external zone; light shading: internal zone; dark shading: northern and south-western zones with radial lineations (refer text for explanations).

bands should, therefore, be related to deformation of the magmas during their emplacement. It should be noted here that in between the bifurcated bands, there is a low anisotropy corridor parallel to the pluton axis and to the NW–SE lineation trend.

3. The Ppara% values ranging between 2 and 5% represent half of the stations and are well distributed amongst all the lithologies. Finally, the lowest Ppara% values (<2%) mainly correspond to the monzogranites and to the hybrid diorites containing rounded mafic enclaves, indicating a weak finite deformation (Fig. 5d, marked in Fig. 8a). In contrast, the hybrid diorite facies containing highly stretched mafic enclaves (Fig. 5a–c), have high anisotropies (constituting the bifurcated bands). Therefore, the Ppara% parameter may be a good indicator of the degree of deformation in the intermediate to mafic facies.

4.6. Shape of AMS ellipsoid

The magnetic shape parameter T is used to characterise the shape of the magnetic ellipsoid (Jelinek, 1978; Hrouda, 1982; Borradaile, 1988). T can vary from very planar ($T = +1.0$) to very linear ($T = -1.0$) ellipsoids. This parameter allows the definition of the type of fabric and subsequently the nature of deformation (flattening or stretching).

The Negash pluton displays all types of magnetic fabrics with T varying from −0.68 to 0.92 (Fig. 8b):

1. The very linear ($T < 0$) to linear ($T < 0.2$) fabrics are mainly situated along a corridor that coincides with the axis of the pluton and roughly correspond to low anisotropy values. Very linear fabrics are also represented in the diorites along their contact with the granodiorites, which extends for nearly 5 km in the south-eastern part of the pluton. These fabrics are in strong contrast with the planar fabrics in the adjacent granodiorites.
2. The plano-linear fabrics ($T = 0.2$ to 0.6) characterise the largest part of the pluton.
3. The very planar fabrics ($T > 0.6$) are represented along a NW–SE oriented corridor adjacent to the

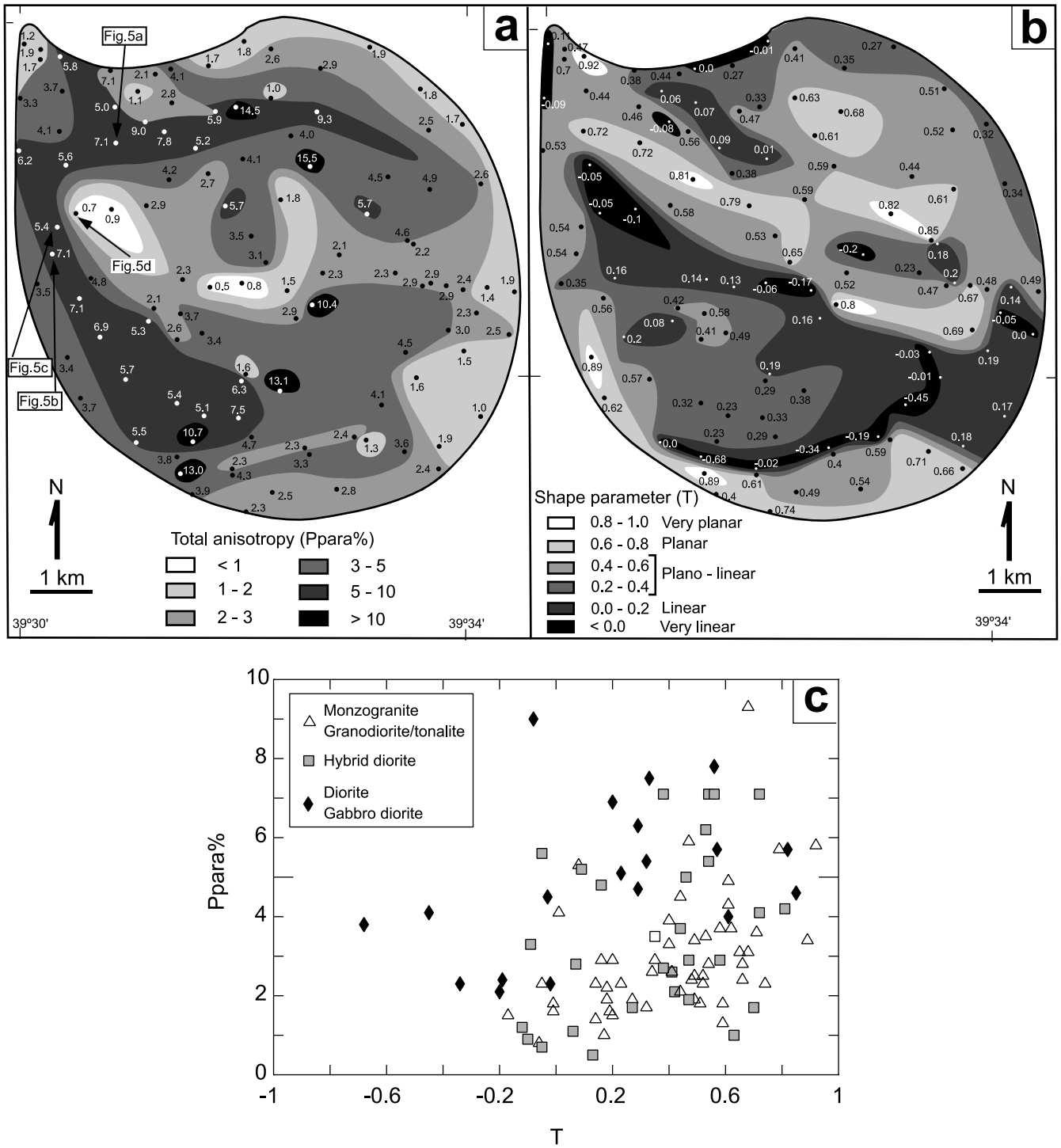

Fig. 8. Scalar AMS parameters in the Negash pluton: (a) magnetic anisotropy (Ppara%); (b) shape parameter (*T*); and (c) Ppara% vs. *T* graph displaying that all the rocks tend to have a more planar fabric with increasing anisotropy.

corridor with linear fabrics, and at the southern border of the pluton. It should be remarked that the fabric along the south-eastern border becomes more linear and then progressively more planar towards the northern border, although these border zones are all constituted by the same monzogranite. This demonstrates that the shape parameter can be variable within the same lithology, and hence can be used as an indicator of the type of deformation.

Anisotropy vs. shape parameter graph (Fig. 8c) indicates that all the rocks tend to have more planar fabrics with increasing anisotropy.

5. Discussion

5.1. Interpretation of pluton structures

Magnetic fabrics checked against field data show consistent patterns (Figs. 6 and 7). This fact, along with the distribution of the various orientations of foliation and lineation with respect to their position in the pluton and with respect to rock types allowed us to regard our data with some confidence.

The magmatic nature of the microfabrics indicates that the deformation of the magmas took place while they were not entirely crystallized, and that there was no significant post-emplacement deformation. Moreover, the general structural continuity across all the facies suggests that the magmas were deformed contemporaneously during their emplacement. Therefore, it is likely that most of the foliations and lineations reflect magmatic flow, and that their attitude is linked to the interference between regional deformation and ballooning.

The lineations close to the border of the pluton are in most cases sub-horizontal and follow the contour of the pluton (Fig. 7). This peripheral zone roughly corresponds to the felsic facies (Fig. 2). The foliation trajectories are also concentric and sub-parallel to the internal lithological boundaries and to the external pluton border (Fig. 6). These concentric structures at the border of the pluton and the presence of radial dykes may indicate the horizontal stretching and flattening of the magmas due to ballooning (see for instance Vernon and Paterson, 1993).

The lineations in the internal zone of the pluton strike north-west and plunge at moderate angles towards the north-west. These lineations are at high angles to the respective foliations. As the lineation and foliation trajectories converge towards the north-western tip of the pluton, the root zone is not at the centre of the pluton but at its north-western tip.

The significance of the inward plunging radial lineations at the south-western and north-eastern borders of the pluton is not clear (Fig. 7). They may represent a zone where either the ballooning was not so important or the lineations were later reoriented (by the emplacement of the mafic magma batch?). However, since the two zones with radial lineations are nearly symmetrical with respect to the axis of the pluton, this may suggest that the ballooning possibly occurred partly in NE–SW direction.

The obliquity among the superposed magmatic foliations and the septa of the country rocks at the northern and southern borders of the pluton (Fig. 6a), symmetric with respect to the NW–SE pluton axis, also suggests that the magma transfer was from the NW (the likely feeder zone) towards the SE, with a faster lateral expansion to the SE than towards the northern and southern borders.

5.2. Reconstruction of pluton geometry: synthetic cross-sections

Four cross-sections (Fig. 9a), one along the axis of the pluton (NW–SE) and three perpendicular to it (SW–NE), are constructed from the AMS and field structural data. Although it is difficult to reconstruct the attitude of foliations in the root zone of the pluton in the absence of gravity data, extrapolation to depth of the surface dips of both foliations and lineations seems to be the more logical way to gather all the data. Along the NW–SE section (AA′), the foliations in the SE border of the pluton have dips $>50°$ (dipping towards the NW). The dip gradually decreases towards the centre of the pluton ($<50°$), and then increases again to $>60°$ in the NW, where vertical foliations mark the high strain zone in the western border of the pluton. This variation in attitude along the NW–SE section is also true for the lineations. The section also illustrates lithological zonation from SE to NW: monzogranite, granodiorite–tonalite, diorite–gabbrodiorite, granodiorite–tonalite to hybrid diorite. Since these facies form roughly regular arcuate shapes in map view, this regularity in thickness is more or less preserved in the cross-section. All the facies converge at depth towards the NW where the feeder zone is likely situated. The SW–NE sections (BB′, CC′ and DD′) illustrate regular inward foliation. The septa and mafic enclaves follow similar trends. This shows the basin-shaped structure of the pluton along the SW–NE sections with its depth increasing towards the NW.

The combination of the four cross-sections enables one to construct a likely three-dimensional geometry of the pluton below the present level of erosion (Fig. 9b). The pluton has an asymmetric funnel-shaped structure with a feeder zone at the north-western tip of the pluton and is made of four main magma pulses as discussed in the next section. The inward dipping structural trend indicates that the upper half of the pluton has been removed and suggests the roof of the pluton to have likely been much above the present level of exposure.

5.3. South-eastern diorite–granodiorite contact zone

The diorites and granodiorites at the south-eastern part of the pluton are characterised by distinct AMS features across their lower magmatic contact. This contact roughly corresponds to the limit between the circumferential and radial zones of lineations (Fig. 7). The lineations in the granodiorites are sub-horizontal and stretched parallel to the pluton boundary while those in the diorites immediately at the contact are gently plunging towards the north-west. Similarly, the anisotropy and shape parameters are very different. The diorites have relatively lower anisotropy and very linear fabric while the granodiorites have relatively higher anisotropy and planar fabric (Fig. 8). The contrasting structural difference implies a local deformation related to the successive emplacement of these two magmas. The mafic tongue can be considered as the result of laminar flow of a mafic pulse within a partially crystallized granodioritic

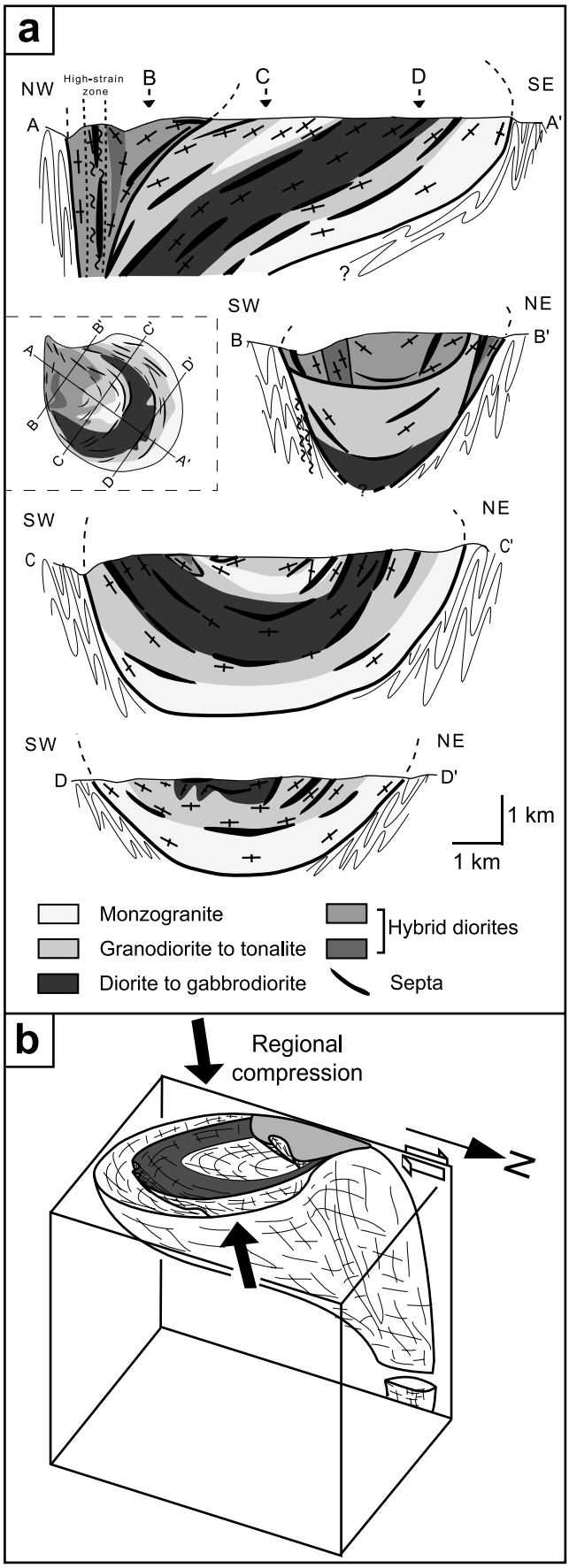

mass. The linear fabrics that reflect syn-emplacement structures in the diorite tongue may reflect flow across the floor of the chamber, and can be attributed to the injection of the dioritic magma into the solidifying and flattening granodioritic magma. The horizontal concentrical lineations in the adjacent monzogranites and granodiorites suggesting circumferential flattening imply that this flow was not permitted but forceful. Moreover, the presence of mafic enclaves within the granodiorites and monzogranites above the mafic mass may suggest subsequent convective stirring above the diorite (Wiebe and Collins, 1998).

Several field observations (Fig. 4) show that the diorite–granodiorite contact is affected by rheological instability, more specifically interfingering of granodiorite lobes into diorites, granitic pipes, and intense mingling at the base of the diorite. Furthermore, the foliation of the diorite is folded in the lobes at the lower contact and the pipes are warped suggesting that the instability developed during emplacement of the dioritic batch. This may be attributed to flow during mafic replenishment (Wiebe and Collins, 1998).

5.4. North-western hybridized diorite zone

The north-western part of the pluton is marked by magnetic susceptibility values intermediate between those of the granodiorites and diorites (Fig. 2). This zone corresponds to the intensively hybridized diorites that form leucocratic to melanocratic masses. Interlayering of mafic–felsic materials, numerous swarms of micro-enclaves with composition similar to the host hybrids, and synplutonic diorite dykes with chilled, lobate and crenulated margins are prominent features of this zone. The magmatic high strain zone at the western border of the pluton with vertical mafic–felsic layering and sub-horizontal lineation and sub-vertical foliation patterns, forms part of the hybrid rocks.

Field relations at the north-western part of the pluton show: (i) mafic–felsic relationships similar to those reported from the south-eastern part of the pluton (Figs. 4 and 5d–f); and (ii) mafic–felsic relationships characterised by a higher mafic/felsic ratio and significant flattening of enclaves (Fig. 5a–c). Since stretched enclaves are observed not only close to but also far from the vertical Suluh shear zone, where they show vertical to oblique (45°) flattening in the latter case, they cannot be considered as the results of only simple deformation due to the shear zone. Moreover, flattened enclaves are found close to undeformed rounded enclaves with no grading in the deformations. Therefore, we suggest that the two types of enclaves observed in the NW reflect two distinct processes of mafic–felsic interactions:

Fig. 9. (a) Synthetic cross-sections. Section AA′ is along the axis of the pluton, the others are perpendicular to AA′. Note the interfingering of the mafic and felsic facies at their contact zone, in section DD′; (b) three-dimensional block diagram of the Negash pluton.

(i) stirring related to mafic replenshiment as observed in the south-eastern contact zone, leading to rounded enclaves within a more or less hybridised matrix (Fig. 5d–f); and (ii) thorough mixing and mingling in a conduit (during ascent) of felsic and mafic magmas leading to stretched enclaves within a hybridised matrix (Fig. 5a–c).

5.5. Model of pluton emplacement and implications to mafic–felsic magma interactions

The pervasive shortening during D_1 deformation of the metavolcanics in the Negash area resulted in the NNE-trending regional foliation. Semi-ductile dextral shear zones developed in the metavolcanics during the subsequent D_2 deformation (Alene, 1996). Such steep shear zones are considered to be suitable to the drainage of magmas (e.g. D'Lemos et al., 1992; Davis, 1993; Ferré et al., 1997) as they are usually continuous at mid- to lower-crustal levels as inclined to sub-horizontal shears (Davies, 1987). The Suluh shear zone (Asrat, 1997) is considered as one such conduit, which possibly acted as a pathway to the successive raising of magmas during a short span of time as evidenced by the magmatic microstructures and contacts.

Our structural data coupled with country rock deformation events call for coeval or a little later emplacement of the Negash pluton with the D_2 semi-ductile dextral shearing event in a transpressive tectonic regime, in the following sequence (Fig. 10):

Stage 1. The regional transpression led to the dextral shearing along the present Suluh shear zone, which was used for the forceful injection of the most buoyant monzogranitic magma using the pre-existing anisotropies of the foliated country rocks. At this stage, the monzogranitic facies emplaced as a sheet with N–S oriented fabrics (later obliterated by ballooning).

Stage 2. Granodioritic magma was intruded into the monzogranitic magma pushing it laterally mainly towards the SE by deflecting the foliation trajectories of the country rocks in the same direction. Near the shear zone, the granodioritic magma was injected as sheets into the foliations of the country rocks. This resulted in the flattening and stretching of these country rocks to form septa. These septa are in continuity with the foliation of the country rocks in the north and south, and they were progressively curved towards the SE at the centre of the pluton.

Stage 3. Dioritic magma was injected into the granodiorite–monzogranite complex while the process of expansion and gradual increment in size of the pluton continued. The abundance of flattened mafic enclave swarms in the host felsic facies, the inter-fingering of the diorites into the granodiorites and the conspicuous mingling features at their contacts suggest their successive but nearly contemporaneous emplacement by the forceful injection of a diorite tongue into the granodioritic magma (e.g. Didier and Barbarin, 1991 and references therein; Michael, 1991; Wiebe and Collins, 1998). The

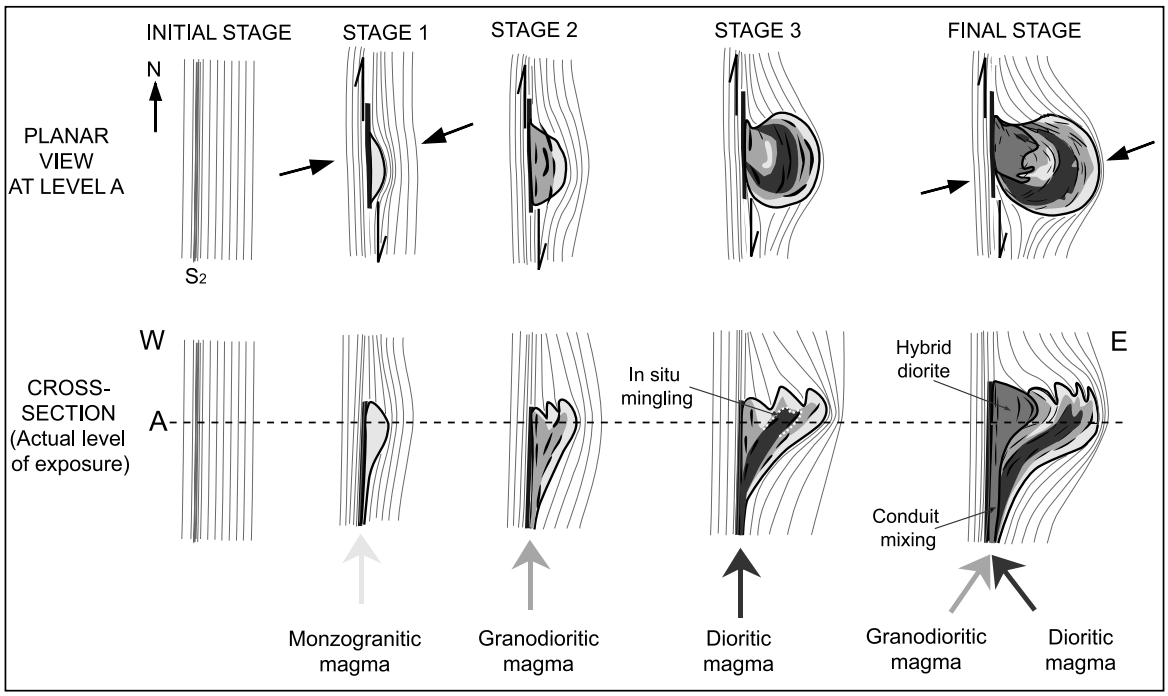

Fig. 10. Model of emplacement of the Negash pluton and mafic–felsic magma interactions. The stripped lines during the initial stage represent the S_2 foliation trajectories in the country rocks. The mingled zones at the contacts are marked by the broken white line in the vertical section of stage 3 at the diorite–granodiorite contact. In the planar view, black arrows represent the direction of compression; dark half-arrows represent the dextral sense of shear. The dark straight lines at the western border of the pluton represent the Suluh shear zone in the country rocks.

emplacement was accompanied by instabilities at the lower interface as evidenced by extensive mingling among the magmas. A small triple point in the country rocks was formed at the southern border of the pluton due to its lateral expansion. Similarly, because of the dextral transpressive component of the regional stress field, the magma was deformed in the western part close to the dextral Suluh shear zone resulting in a beak-shaped form at its north-western tip.

Final stage. A hybridized dioritic magma was emplaced at the western part, pushing the previously emplaced batches further to the east, resulting in the present shape of the whole pluton. The simultaneous mixing, mingling and enclave stretching suggest a dynamic two-way conduit mixing process. The hybridization took place between granodioritic and dioritic magmas drained simultaneously through the same conduit. These two magmas could be either from the same magma chamber at the end of its emptying or from two different chambers. Similar processes have been described elsewhere (e.g. Castro et al., 1995).

6. Conclusions

The AMS study on the Negash pluton reveals petrological zonation, internal structures and mafic–felsic magma interactions. The pluton that was considered to be post-tectonic turned out to be late-tectonic, as evidenced by the conformity of the magmatic and regional Pan-African structures. Interpretation of within pluton and regional structures suggests an emplacement in relation to transpressional tectonic regime with a dextral component along a shear zone during the late Pan-African orogeny. The structures recorded in the pluton are snapshots of the last deformation event in the Pan-African orogeny and indicate the ceasing of any major deformation after its emplacement.

The linear and planar structures allowed the geometry of the pluton and its mode of emplacement to be constrained. Accordingly, the pluton was assembled by successive injection of four magma pulses through an off-centre feeder zone at the north-western tip close to the Suluh shear zone, and by subsequent expansion towards the SE.

Two major types of mafic–felsic magma interactions are recognised: (i) in situ mingling and mixing of the diorites and granodiorites along their contacts, attributed to forceful injection of the dioritic magma into the felsic magmas, and to subsequent mingling/mixing related to instability of the lower interface and convective stirring at the upper interface; and (ii) simultaneous rising of dioritic and granodioritic magmas through the same conduit.

Acknowledgements

We are grateful to J.L. Bouchez who provided us with the AMS facilities at the Laboratory of Petrophysics and Tectonics, Toulouse. Our sincere gratitude goes to Nardos T., Yemane T., Hailu D., and Yonas for their invaluable assistance during the field work. We thank R.A. Wiebe and an anonymous reviewer for their critical reviews that improved the original manuscript. This work was supported by a Ph.D. research grant to A.A. from the French Ministry of Foreign Affairs and financial support from INSU-Ethiopie 2000 Project. We would like to acknowledge the Department of Geology and Geophysics, Addis Ababa University, and Mr and Mrs Vilain for logistical support during the field work. CRPG contribution no. 1624.

References

Alemu, T., 1998. Geochemistry of Neoproterozoic granitoids from the Axum Area, northern Ethiopia. Journal of African Earth Sciences 27, 437–460.

Alene, M., 1996. Some aspects of the geology and structure of the basement rocks in the Maikenetal–Negash area, Northern Ethiopia. Abstract in IGCP Project 348 (the Mozambique and related orogenies). International Field Conference, Northern Ethiopia and Eritrea, March 15–25, 1996.

Almond, D.C., 1983. The concepts of the "Pan-African Episode" and "Mozambique Belt" in relation to the geology of East and Northeast Africa. Bulletin of Faculty Earth Sciences King Abdulaziz University 6, 71–78.

Archanjo, C.J., 1993. Fabriques de plutons granitiques et déformation crustale du Nord-Est du Brésil: une étude par l'anisotropie de la susceptibilité magnétique de granites ferromagnétiques. Unpublished thesis, Université de Paul-Sabatier, Toulouse, France, 167pp.

Archanjo, C.J., Bouchez, J.L., Corsini, M., Vauchez, A., 1994. The Pombal granite pluton: magnetic fabric, emplacement and relationships with the Brasiliano strike-slip setting of NE Brazil (Paraiba State). Journal of Structural Geology 16, 323–335.

Archanjo, C.J., Launeau, P., Bouchez, J.L., 1995. Magnetic fabric vs. magnetite and biotite shape fabrics of the magnetite-bearing granite pluton of Gameleias (Northeast Brazil). Physics of Earth and Planetary Interiors 89, 63–75.

Asrat, A., 1997. Geology and geochemistry of the Negash Pluton and their metallogenic significance, Central Tigrai. Unpublished M.Sc. thesis, Addis Ababa University, Ethiopia, 159pp.

Asrat, A., Barbey, P., Gleizes, G., 2001. The Precambrian geology of Ethiopia: a review. Africa Geoscience Review 18, 271–288.

Barbarin, B., 1988. Field evidence for successive mixing and mingling between the Piolard Diorite and the Saint-Julien-la-Vetre Monzogranite (Nord-Forez, Massif Central, France). Canadian Journal of Earth Sciences 25, 49–59.

Bateman, R., 1995. The interplay between crystallization, replenishment and hybridization in large felsic magma chambers. Earth Science Review 39, 91–106.

Benn, K., Rochette, P., Bouchez, J.L., Hattori, K., 1993. Magnetic susceptibility, magnetic mineralogy and magnetic fabrics in a late Archaean granitoid–gneiss belt. Precambrian Research 63, 59–81.

Beyth, M., 1972. The geology of Central and Western Tigrai. Ph.D. thesis, Rheinische Friedrich-Wilhems Universität, Bonn, W. Germany, 200pp.

Borradaile, G.J., 1988. Magnetic susceptibility, petrofabrics and strain. Tectonophysics 156, 1–20.

Bouchez, J.L., 1997. Granite is never isotropic: an introduction to AMS studies of granitic rocks. In: Bouchez, J.L., Hutton, D.H.W., Stephens, W.E. (Eds.), Granite: from Segregation of Melt to Emplacement Fabrics, Kluwer Academic Publishers, Dordrecht, pp. 95–112.

Bouchez, J.L., Guillet, P., Chevalier, F., 1981. Structures d'écoulement liées à la mise en place du granite de Guérande (Loire-Atlantique, France). Bulletin de la Sociéité géologique de France 23, 387–399.

Bouchez, J.L., Delas, C., Gleizes, G., Nédélec, A., Cuney, M., 1992. Submagmatic microfractures in granites. Geology 20, 35–38.

Bouchez, J.L., Hutton, D.H.W., Stephens, W.E. (Eds.), 1997. Granite: from Segregation of Melt to Emplacement Fabrics. Kluwer Academic Publishers, Dordrecht, 356pp.

Castro, A., De la Rosa, J.D., Fernandéz, C., Moreno-Ventas, I., 1995. Unstable flow, magma mixing and magma-rock deformation in a deep-seated conduit: the Gil-Marquez Complex, south-west Spain. Geologische Rundschau 84, 359–374.

D'Lemos, R.S., Brown, M., Strachan, R.A., 1992. Granite magma generation, ascent and emplacement in a transpressional orogen. Journal of Geological Society of London 149, 487–490.

Davies, G.H., 1987. A shear-zone model for the structural evolution of metamorphic core complexes in south-eastern Arizona. In: Coward, M.P., Dewey, J.F., Hancock, P.L. (Eds.), Continental Extensional Tectonics. Geological Society Special Publications, London, pp. 247–266.

Davis, B.K., 1993. Mechanism of emplacement of the Cannibal Creek Granite with special reference to timing and deformation history of the aureole. Tectonophysics 224, 337–362.

Déléris, J., Nédélec, A., Ferré, E., Gleizes, G., Ménot, R.P., Obasi, C.K., Bouchez, J.L., 1996. The Pan-African Toro Complex (Northern Nigeria): magmatic interactions and structures in a bimodal intrusion. Geology Magazine 133, 535–552.

Didier, J., Barbarin, B. (Eds.), 1991. Enclaves and Granite Petrology. Elsevier Science Publishers, Amsterdam, 625pp.

Djouadi, M.T., Gleizes, G., Ferré, E., Bouchez, J.L., Caby, R., Lesquer, A., 1997. Oblique magmatic structures of two epizonal granite plutons, Hoggar, Algeria: late-orogenic emplacement in a transcurrent orogen. Tectonophysics 279, 351–374.

EIGS (Ethiopian Institute of Geological Surveys), 1997. Geological Map of Ethiopia, 1:2,000,000. Ministry of Mines and Energy, Addis Ababa.

Fernandez, A., Gasquet, D., 1994. Relative rheological evolution of chemically contrasted coeval magmas- example of the Tichka plutonic complex (Morocco). Contributions to Mineralogy and Petrology 116, 316–326.

Ferré, E., Gleizes, G., Bouchez, J.L., Nnabo, P.N., 1995. Internal fabric and strike-slip emplacement of Solli Hills, northern Nigeria. Tectonics 14, 1205–1219.

Ferré, E., Gleizes, G., Djouadi, M.T., Bouchez, J.L., 1997. Drainage and emplacement of magmas along transcurrent shear zone: petrophysical evidence from a granite–charnockite pluton (Rhama, Nigeria). In: Bouchez, J.L., Hutton, D.H.W., Stephens, W.E. (Eds.), Granite: from Segregation of Melt to Emplacement Fabrics, Kluwer Academic Publishers, Dordrecht, pp. 253–274.

Ferré, E., Gleizes, G., Caby, R., 2002. Obliquely convergent tectonics and granite emplacement in the Trans-Saharan belt of Eastern Nigeria: a synthesis. Precambrian Research 144, 199–219.

Garland, C.R., 1980. Geology of the Adigrat Area. Memoir No. 1. Ministry of Mines and Energy, Addis Ababa, Ethiopia. 51pp.

Gleizes, G., Nédélec, A., Bouchez, J.L., Autran, A., Rochette, P., 1993. Magnetic susceptibility of the Mont-Louis-Andorra ilmenite type granite (Pyrenees): a new tool for the petrographic characterization and the regional mapping of zoned granite plutons. Journal of Geophysical Research 98, 4317–4331.

Gleizes, G., Leblanc, D., Santana, V., Olivier, P., Bouchez, J.L., 1998. Sigmoidal structures featuring dextral shear during emplacement of the Hercynian granite complex of Cauterets-Panticosa (Pyrenees). Journal of Structural Geology 20, 1229–1245.

Gleizes, G., Leblanc, D., Olivier, P., Bouchez, J.L., 2001. Strain partitioning in a pluton during emplacement in transpressional regime: the example of the Néouvielle granite (Pyrenees). Geologische Rundschau 90, 325–340.

Grégoire, V., Darrozes, P., Gaillot, P., Nédélec, A., Launeau, P., 1998. Magnetite grain shape fabric and distribution anisotropy vs. rock magnetic fabric: a three-dimensional case study. Journal of Structural Geology 20, 937–944.

Hrouda, F., 1982. Magnetic anisotropy of rocks and its application in geology and geophysics. Geophysical Survey 5, 37–82.

Jelinek, V., 1978. Statistical processing of anisotropy of magnetic susceptibility measured on groups of specimens. Studies of Geophysics and Geodynamics 22, 50–62.

Kazmin, V., 1972. Geological map of Ethiopia. Ministry of Mines and Energy, 1:2,000,000. Addis Ababa, Ethiopia.

Kröner, A., Greiling, R., Reischmann, T., Hussein, I.M., Stern, R.J., Dur, S., Kruger, J., Zimmer, M., 1987. Pan-African crustal evolution in the Nubian segment of north-eastern Africa. In: Kröner, A. (Ed.), Proterozoic Lithospheric Evolution. American Geophysical Union, Geodynamic Series 15, pp. 235–257.

Kröner, A., Stern, R.J., Linnebacker, P., Manton, W., Reischmann, T., Hussein, I.M., 1991. Evolution of Pan-African island arc assemblages in the south Red Sea hills, Sudan and SW Arabia as exemplified by geochemistry and geochronology. Precambrian Research 53, 99–118.

McNulty, B.A., Tobisch, O.T., Cruden, A.R., Stuart, G., 2000. Multistage emplacement of the Mount Givens pluton, central Sierra Nevada batholith, California. Geological Society of America Bulletin 112, 119–135.

Michael, P.J., 1991. Intrusion of basaltic magma into a crystallizing granitic magma chamber: the Cordillera del Paine pluton in Chile. Contributions to Mineralogy and Petrology 108, 396–418.

Miller, J.A., Mohr, P.A., Rogers, A.S., 1967. Some new K–Ar age determinations of basement rocks from Eritrea. Bulletin of Geophysical Observatory, Addis Ababa University 10, 53–57.

Mock, C., Arnaud, N.O., Cantagrel, J.M., Yirgu, G., 1999. $^{40}Ar/^{39}Ar$ Thermochronology of the Ethiopian and Yemeni basements: reheating related to the Afar plume. Tectonophysics 314, 351–372.

Nédélec, A., Paquette, J.L., Bouchez, J.L., Olivier, P., Railson, B., 1994. Stratoid granites of Madagascar: structure and position in the Pan-African orogeny. Geodinamica Acta 7, 48–56.

Oldenburg, C.M., Spera, F.J., Yuen, D.A., Sewell, G., 1989. Dynamic mixing in magma bodies: theory, simulations and implications. Journal of Geophysical Research 94, 9215–9236.

Paterson, S.R., Vernon, R.H., Tobisch, O.T., 1989. A review of criteria for the identification of magmatic and tectonic foliations in granitoids. Journal of Structural Geology 11, 349–363.

Poli, G., Tommasini, S., 1999. Geochemical modelling of acid–basic magma interaction in the Sardinia–Corsica Batholith: the case study of Sarrabus, south-eastern Sardinia, Italy. Lithos 46, 553–571.

Reid, J.B., Evans, O.C., Fates, D.G., 1983. Magma mixing in granitic rocks of the central Sierra Nevada, California. Earth and Planetary Science Letters 66, 243–261.

Rochette, P., Jackson, M., Aubourg, C., 1992. Rock magnetism and the interpretation of anisotropy of magnetic susceptibility. Reviews of Geophysics 30, 209–226.

Saint-Blanquat de, M., Tikoff, B., 1997. Development of magmatic to solid state fabrics during syntectonic emplacement of the Mono Creek granite, Sierra Nevada batholith. In: Bouchez, J.L., Hutton, D.H.W., Stephens, W.E. (Eds.), Granite: from Segregation of Melt to Emplacement Fabrics, Kluwer Academic Publishers, Dordrecht, pp. 231–252.

Seaman, S.J., Scherer, E.E., Standish, J.J., 1995. Multistage magma mingling and the origin of flow banding in the Aliso lava dome, Tumacacori Mountains, southern Arizona. Journal of Geophysical Research 100, 8381–8398.

Snyder, D., Tait, S., 1998. The imprint of basalt on the geochemistry of silicic magmas. Earth and Planetary Science Letters 160, 433–445.

Stern, A.J., Dawoud, A.S., 1991. Late Precambrian (740 Ma) charnockite, enderbite, and granite from Jebel Moya, Sudan: a link between the Mozambique Belt and the Arabian–Nubian Shield? Geology 99, 648–659.

Stern, R.J., 1994. Arc assembly and continental collision in the

Neoproterozoic East African Orogen: implications for the consolidation of Gondwanaland. Annual Reviews Earth Planetary Sciences 22, 319–351.

Tadesse, T., 1997. The Geology of Axum Area (ND 37-6), Memoir No. 9. Ethiopian Institute of Geological Surveys, Addis Ababa, Ethiopia, 184pp.

Tadesse, T., Hoshino, M., Sawada, Y., 1999. Geochemistry of low-grade metavolcanic rocks from the Pan-African of the Axum Area, northern Ethiopia. Precambrian Research 99, 101–124.

Tadesse, T., Hoshino, M., Suzuki, K., Iizumi, S., 2000. Sm–Nd, Rb–Sr and Th–U–Pb zircon ages of syn- and post- tectonic granitoids from the Axum area of northern Ethiopia. Journal of African Earth Sciences 30, 313–327.

Vernon, R.H., Etheridge, M.A., Wall, V.J., 1988. Shape and microstructure of microgranitoid enclaves: indicators of magma mingling and flow. Lithos 22, 1–11.

Vernon, R.H., Paterson, S.R., 1993. The Ardara pluton, Ireland: deflating an expanded intrusion. Lithos 31, 17–32.

Weinberg, R.F., 1997. The disruption of a diorite magma pool by intruding granite: the Sobu body, Ladakh Batholith, Indian Himalayas. Journal of Geology 105, 87–98.

Weinberg, R.F., Leitch, A.M., 1998. Mingling in mafic magma chambers replenished by light felsic inputs: fluid dynamical experiments. Earth and Planetary Science Letters 157, 41–56.

Whalen, J.B., Currie, K.L., 1984. The Topsails igneous terrane, Western Newfoundland: evidence for magma mixing. Contributions to Mineralogy and Petrology 87, 319–327.

Wiebe, R.A., 1987. Rupture and inflation of a basic magma chamber by silicic liquid. Nature 326, 69–71.

Wiebe, R.A., 1996. Mafic–silicic layered intrusions: the role of basaltic injections on magmatic processes and the evolution of silicic magma chambers. Transactions of the Royal Society of Edinburgh: Earth Sciences 87, 233–242.

Wiebe, R.A., Wild, T., 1983. Fractional crystallization and magma mixing in the Tigalak layered intrusion, the Nain anorthosite complex, Labrador. Contributions to Mineralogy and Petrology 84, 327–344.

Wiebe, R.A., Adams, S.D., 1997. Felsic enclave swarms in the Gouldsboro granite, Coastal Maine: a record of eruption through roof of a silicic magma chamber. Journal of Geology 105, 617–627.

Wiebe, R.A., Collins, W.J., 1998. Depositional features and stratigraphic sections in granitic plutons: implications for the emplacement and crystallization of granitic magma. Journal of Structural Geology 20, 1273–1289.

Zorpi, M.J., Coulon, C., Orsini, J.B., Cocirta, C., 1989. Magma mingling, zoning and emplacement in calc-alkaline granitoid plutons. Tectonophysics 157, 315–329.